

Tuning Nonlinear Elastic Materials under Small and Large Deformations

HUANYU CHEN, University of Southern California, USA
 JERNEJ BARBIČ, University of Southern California, USA

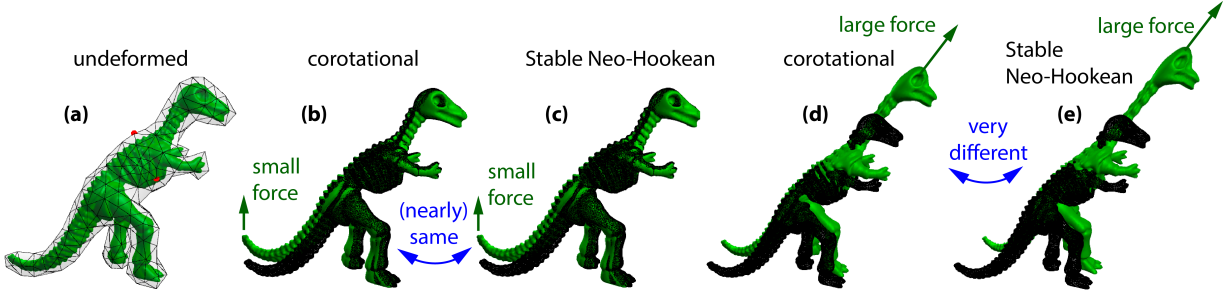


Fig. 1. **Volumetric material normalization.** We compare a corotational solid volumetric material [Müller and Gross 2004] against the Stable Neo-Hookean (SNH) material [Smith et al. 2018] (elastic energy functions are given in Table 1). Red vertices are constrained (a). Observe that for SNH, $\lambda_{\text{Lamé}} = \lambda - \mu$, $\mu_{\text{Lamé}} = \mu$, where λ, μ are the SNH material parameters (Table 1), but for corotational material, $\lambda_{\text{Lamé}} = \lambda$, $\mu_{\text{Lamé}} = \mu$. If one naively uses SNH and misidentifies the SNH parameter λ as $\lambda_{\text{Lamé}}$, the resulting stiffness matrix in the undeformed shape differs from that of the corotational material. The frequencies of the resulting linear vibrational modes also mismatch; at $\nu = 0.2$, the lowest frequency is off by 18%. Instead, given any particular desired E and ν , we determine $\lambda_{\text{Lamé}}$ and $\mu_{\text{Lamé}}$ using Equation 15. We then solve for λ and μ , separately for SNH and corotational, using Table 1. The result is that now both materials have the same stiffness matrix (and mass matrix) in the rest shape; this is already predicted by our theory, but we also checked it experimentally. Effectively, this means that we “normalized” SNH to match the corotational material under small deformations. Consequently, for small loads, the two materials produce almost the same output (b,c). We can then observe the difference between these two materials due to the nonlinearities; they are revealed under large forces (d,e).

In computer graphics and engineering, nonlinear elastic material properties of 3D volumetric solids are typically adjusted by selecting a material family, such as St. Venant Kirchhoff, Linear Corotational, (Stable) Neo-Hookean, Ogden, etc., and then selecting the values of the specific parameters for that family, such as the Lamé parameters, Ogden exponents, or whatever the parameterization of a particular family may be. However, the relationships between those parameter values, and visually intuitive material properties such as object’s “stiffness”, volume preservation, or the “amount of nonlinearity”, are less clear and can be tedious to tune. For an arbitrary isotropic hyperelastic energy density function ψ that is not parameterized in terms of the Lamé parameters, it is not even clear what the Lamé parameters and Young’s modulus and Poisson’s ratio are. Starting from ψ , we first give a concise definition of Lamé parameters, and therefore Young’s modulus and Poisson’s ratio. Second, we give a method to adjust the object’s three salient properties, namely two small-deformation properties (overall “stiffness”, and amount of volume preservation, prescribed by object’s Young’s modulus and Poisson’s ratio), and one large-deformation property (material nonlinearity). We do this in a manner whereby each of these three properties is decoupled from the other two properties, and can therefore be set independently. This permits a new ability, namely “normalization” of materials: starting from two distinct materials, we can “normalize” them so that they have the same small deformation properties, or the same large-deformation nonlinearity behavior, or both. Furthermore, our analysis produced a useful theoretical result, namely it establishes that Linear Corotational materials (arguably the most widely used materials in computer graphics) are the simplest possible nonlinear materials.

CCS Concepts: • **Computing methodologies** → **Physical simulation.**

Additional Key Words and Phrases: nonlinear materials, FEM, first Piola-Kirchhoff stress, corotational material

Authors’ addresses: Huanyu Chen, University of Southern California, Los Angeles, USA, huanyuc@usc.edu; Jernej Barbič, University of Southern California, Los Angeles, USA, jnb@usc.edu.

1 INTRODUCTION

Adjusting deformable object material properties to meet some artistic goal is a commonly encountered operation in computer graphics practice. There is a plethora of available material model families, each of which incorporates a small number of material parameters to tune. When investigating all these materials, it is useful to be able to ensure that the materials all share the same small deformation properties, so that the differences in their large-deformation nonlinear properties can be investigated systematically against a common small deformation baseline. By small deformation properties, we mean the material’s two Lamé parameters, or equivalently (via bijective formulas), Young’s modulus and Poisson’s ratio. While many material families do already parameterize the materials via Lamé parameters, this is not universally true. And so the first question that we address is, “Is it possible to meaningfully *define* Lamé parameters (and consequently Young’s modulus and Poisson’s ratio) for an arbitrary isotropic hyperelastic nonlinear material? We provide such a definition in this paper, and it matches the Lamé parameters for the common materials. The key idea is to perform a second-order Taylor expansion of ψ in terms of λ_i around the rest shape ($\lambda_i = 1$, $i = 1, 2, 3$). This process is identical to approximating the first Piola-Kirchhoff (PK1) principal stresses (singular values of the PK1 tensor $P = d\psi/dF$; F is the 3×3 deformation gradient) at the rest shape as a linear function of λ_i , a process that we call PK1-linearization. PK1-linearization correctly incorporates rotations, and as such does not suffer from artifacts under large deformations. Note that in deformable object modeling, a more common linearization is the one of internal forces around the rest shape using the stiffness matrix; however, this linearization is not rotation-invariant and quickly produces visible artifacts. We prove that for any ψ , its

PK1-linearization is a Linear Corotational material. Obviously, any Linear Corotational material is a PK1-linearization of at least one material, namely itself. This means that Linear Corotational materials are “special”, namely they are precisely the materials that do not have any third-order or higher terms in their Taylor expansion in terms of λ_i around the rest shape. This sheds a new light on this widely used material: in light of our result, the popularity of Linear Corotational materials is not surprising; they are arguably the simplest possible nonlinear isotropic materials. These observations also lead to a natural definition of Lamé parameters for an arbitrary ψ . Namely, compute the Linear Corotational material that is its PK1-linearization, and read the Lamé parameters of that material. These observations allow us to find a material in any material family (with at least two parameters) that matches a given Young’s modulus and Poisson’s ratio. They also allow us to “normalize” two nonlinear materials so that they have the same quadratic Taylor expansion (or equivalently, PK1-linearization), i.e., they share the same Lamé parameters, or equivalently Young’s modulus or Poisson’s ratio.

With the small-deformation regime covered, we then propose a method to modify any material ψ so that (1) its PK1-linearization remains the same, and (2) the material progressively stiffens or softens under large deformations in a prescribed manner, using a single scalar parameter that we call “nonlinearity”. This makes it easily possible to make a material more or less nonlinear. An existing alternative is to change the material family for one that is inherently more (or less) nonlinear (e.g., StVK is known to be more nonlinear than the Stable Neo-Hookean material). However, this still limits the choice to a few discrete material families; whereas with our method, we obtain a continuously-varying nonlinearity adjustment.

2 RELATED WORK

Our work is applicable generally to 3D solid deformable object simulation; it acts as a mechanism to adjust the material properties to meet specific user requirements, and is agnostic of the specific underlying simulator. Nonlinear deformable object simulation has a long history in computer graphics; for good surveys, please see [Kim and Eberle 2020; Sifakis and Barbič 2012]. We use “stretch-based” materials [Chen et al. 2023; Xu et al. 2015] to express the elastic energy density function. These are materials where the elastic energy density function is an isotropic function of the three principal stretches; we use them because they are general, and recent work demonstrated how to robustly remove singularities [Chen et al. 2023]. Designing 3D solid material properties to meet specific artistic goals has been investigated in [Wang et al. 2020]; however, the paper only discussed adjusting “stiffness” (via Young’s modulus); and did not discuss Poisson’s ratio, Lamé parameters or nonlinearity adjustments. For plants [Wang et al. 2017], it has been shown how to adjust model-reduced models to match desired user frequencies. There has not been a prior method that has demonstrated how to adjust nonlinearity and small-deformation behavior with only three compact continuous parameters. The definitions of “PK1-linearity” and the observations and proofs on the special role of the Linear Corotational material are also novel. Linear Corotational material has been introduced to computer graphics in [Müller and Gross

2004], and is widely used, e.g., [Arriola-Rios et al. 2020; Chao et al. 2010; Hecht et al. 2012; McAdams et al. 2011; Verschoor et al. 2018].

There are many nonlinear material models used in computer graphics and engineering. Our method is generic and works with an arbitrary isotropic material. We explicitly provide our defined and computed Lamé parameters (Table 1) for many commonly used materials. These include materials from the Seth-Hill family [Seth 1964] (Linear Corotational, StVK, Hencky, Symmetric Seth-Hill [Bazant 1998], Hill family [Hill 1968]); Neo-Hookean materials (standard Neo-Hookean, Stable Neo-Hookean [Smith et al. 2018], STS [Pai et al. 2018]); Valanis-Landel materials [Peng and Landel 1972; Valanis and Landel 1967; Valanis 2022; Xu et al. 2015]; materials used in geometric modeling (ARAP [Sorkine and Alexa 2007], Symmetric ARAP [Shtengel et al. 2017], Symmetric Dirichlet [Smith and Schaefer 2015]); and Ogden [Ogden 1972] and Mooney-Rivlin materials. For a comprehensive review of isotropic hyperelastic material models, please refer to [Beda 2014; He et al. 2022; Melly et al. 2021].

3 PK1-LINEARIZATION OF ISOTROPIC MATERIALS

What happens if we approximate a 3D isotropic hyperelastic material elastic energy density function $\psi(\lambda_1, \lambda_2, \lambda_3)$ up to the second order around the rest shape in terms of $\lambda_1, \lambda_2, \lambda_3$? This question is important because such an approximation controls the small-deformation behavior, while still resulting in a nonlinear simulation that does not exhibit artifacts under large deformations, as explained below. Equivalently, this can be seen as a linearization of the first Piola-Kirchhoff (PK1) principal stresses $p_i = \partial\psi/\partial\lambda_i \in \mathbb{R}$ around the rest shape in terms λ_i . Recall that the PK1 stress tensor $P \in \mathbb{R}^{3 \times 3}$ is computed as [Irving et al. 2004; Teran et al. 2005]

$$P = U \text{diag}\left(p_1(\lambda_1, \lambda_2, \lambda_3), p_2(\lambda_1, \lambda_2, \lambda_3), p_3(\lambda_1, \lambda_2, \lambda_3)\right) V^T, \quad (1)$$

$$\text{for } F = U \text{diag}\left(\lambda_1, \lambda_2, \lambda_3\right) V^T, \quad (2)$$

where $F \in \mathbb{R}^{3 \times 3}$ is the deformation gradient, $U, V \in \mathbb{R}^{3 \times 3}$ are orthogonal matrices from the SVD of F , $\lambda_i \in \mathbb{R}$ are the singular values of F (the “principal stretches”), and $p_i = \partial\psi/\partial\lambda_i \in \mathbb{R}$ are the *principal* PK1 stresses, i.e., singular values of P . Because of the presence of U and V , if we linearize the PK1 principal stresses in terms of λ_i (or equivalently, approximate ψ up to second order in terms of λ_i), the simulation remains rotation-aware and will not exhibit geometric linearity artefacts. The PK1-linearization is governed by two linear parameters (Young’s modulus E , Poisson’s ratio ν) or equivalently, $(\lambda_{\text{Lamé}}, \mu_{\text{Lamé}})$, as established by the following theorem.

THEOREM 3.1. *The 2nd-order Taylor expansion of any 3D isotropic hyperelastic volumetric material ψ as a function of principal stretches $\lambda_1, \lambda_2, \lambda_3$ around the rest shape $\lambda_1 = \lambda_2 = \lambda_3 = 1$ is a Linear Corotational material. The Lamé parameters of this Linear Corotational material are a unique function of ψ , as follows:*

$$\lambda_{\text{Lamé}} = \partial_{12}\psi(1, 1, 1), \quad (3)$$

$$\mu_{\text{Lamé}} = \frac{1}{2}(\partial_{11}\psi(1, 1, 1) - \partial_{12}\psi(1, 1, 1)). \quad (4)$$

PROOF. The 2nd-order Taylor expansion of $\psi(\lambda_1, \lambda_2, \lambda_3)$ around $(1, 1, 1)$ is

$$\psi(1, 1, 1) + \sum_{i=1}^3 \partial_i \psi(1, 1, 1)(\lambda_i - 1) + \frac{1}{2} \sum_{i=1}^3 \partial_{ij} \psi(1, 1, 1)(\lambda_i - 1)(\lambda_j - 1), \quad (5)$$

where

$$\partial_i \psi = \frac{\partial \psi}{\partial \lambda_i}, \quad \partial_{ij} \psi = \frac{\partial^2 \psi}{\partial \lambda_i \partial \lambda_j}. \quad (6)$$

Because $\psi(1, 1, 1) = 0$ and $\partial_i \psi(1, 1, 1) = 0$, for $i = 1, 2, 3$, the 0th-order and the 1st-order terms disappear. The 2nd-order term can be further simplified since ψ is a symmetric function of $\lambda_1, \lambda_2, \lambda_3$,

$$\partial_{11} \psi(1, 1, 1) = \partial_{22} \psi(1, 1, 1) = \partial_{33} \psi(1, 1, 1), \quad (7)$$

$$\partial_{12} \psi(1, 1, 1) = \partial_{13} \psi(1, 1, 1) = \partial_{23} \psi(1, 1, 1), \quad (8)$$

It follows that

$$\frac{1}{2} \sum_{i=1}^3 \partial_{ij} \psi(1, 1, 1)(\lambda_i - 1)(\lambda_j - 1) = \quad (9)$$

$$= \frac{1}{2} \partial_{11} \psi(1, 1, 1)((\lambda_1 - 1)^2 + (\lambda_2 - 1)^2 + (\lambda_3 - 1)^2) + \partial_{12} \psi(1, 1, 1)((\lambda_1 - 1)(\lambda_2 - 1) + (\lambda_1 - 1)(\lambda_3 - 1) + (\lambda_2 - 1)(\lambda_3 - 1)) = \quad (10)$$

$$= \frac{1}{2} (\partial_{11} \psi(1, 1, 1) - \partial_{12} \psi(1, 1, 1))((\lambda_1 - 1)^2 + (\lambda_2 - 1)^2 + (\lambda_3 - 1)^2) + \frac{1}{2} \partial_{12} \psi(1, 1, 1)(\lambda_1 + \lambda_2 + \lambda_3 - 3)^2. \quad (11)$$

But, this is exactly the Linear Corotational material with

$$\lambda_{\text{Lamé}} = \partial_{12} \psi(1, 1, 1), \quad (12)$$

$$\mu_{\text{Lamé}} = \frac{1}{2} (\partial_{11} \psi(1, 1, 1) - \partial_{12} \psi(1, 1, 1)). \quad (13)$$

□

The theorem implies that the behavior of any volumetric solid isotropic material around the rest shape is determined by two quantities $\partial_{11} \psi(1, 1, 1)$ and $\partial_{12} \psi(1, 1, 1)$, and they provide the *quadratic expansion* of the material. Therefore, this enables us to *define* the Lamé parameters of an arbitrary volumetric isotropic material $\psi(\lambda_1, \lambda_2, \lambda_3)$ using the formulas in Equation 3 and 4! Note that several (but not all) popular material families are already defined in terms of Lamé parameters; for those families our definition above matches those Lamé parameters. In Section 4, we give a comprehensive table listing the two Lamé parameters for many commonly used materials. Even though two volumetric materials may be distinct and even exhibit very different behavior under large deformations, their PK1-linearization behavior is characterized by the above-defined $\mu_{\text{Lamé}}$ and $\lambda_{\text{Lamé}}$. This observation enables us to “normalize” nonlinear volumetric elastic materials so that their behavior around the rest shape is the same. Therefore, their differences under large deformations can be more meaningfully compared. We show an example of such a process in Figure 1.

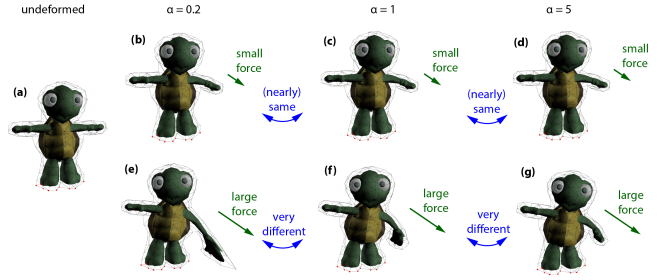


Fig. 2. **By adjusting α , the deformable object can be made more or less stiff under large deformations.** The small deformation behavior is unchanged when changing α .

4 NORMALIZATION OF 3D VOLUMETRIC MATERIALS

Table 1 gives the PK1-linearizations for several common 3D volumetric materials. For volumetric solids, we can compute Young’s modulus E and Poisson’s ratio ν as

$$E = \frac{\mu_{\text{Lamé}}(3\lambda_{\text{Lamé}} + 2\mu_{\text{Lamé}})}{\lambda_{\text{Lamé}} + \mu_{\text{Lamé}}}, \quad \nu = \frac{\lambda_{\text{Lamé}}}{2(\lambda_{\text{Lamé}} + \mu_{\text{Lamé}})}. \quad (14)$$

Therefore, Ogden, ARAP, Symmetric ARAP and Symmetric Dirichlet have $\nu = 0$ (i.e., there is no volume preservation); for these materials, we have $E = 2\mu_{\text{Lamé}}$. Often in computer graphics and engineering, we want to prescribe the material “stiffness” (via E), and volume preservation (via ν). This can be done using the formulas

$$\lambda_{\text{Lamé}} = \frac{Ev}{(1 + \nu)(1 - 2\nu)}, \quad \mu_{\text{Lamé}} = \frac{E}{2(1 + \nu)}. \quad (15)$$

The next step is then to set the parameters of the specific material (Table 1) to meet this $\lambda_{\text{Lamé}}$ and $\mu_{\text{Lamé}}$. For two-dimensional material families this will lead to a unique solution of the material parameters, as a function of $\lambda_{\text{Lamé}}$ and $\mu_{\text{Lamé}}$. For three or higher-dimensional families, the solution is not unique, but can be biased to prefer modifying only any two particular parameters, or modify all parameters by the least amount, as two possible example approaches.

5 ADJUSTING THE NONLINEARITY

Given any isotropic function ψ that has been processed as explained above (Section 4) to obtain desired linear properties, we now show how to modify its nonlinearity, without changing the linear properties. We do this by modifying $\psi(\lambda_1, \lambda_2, \lambda_3)$ to the function

$$\psi_\alpha(\lambda_1, \lambda_2, \lambda_3) = \frac{1}{\alpha^2} \psi(\lambda_1^\alpha, \lambda_2^\alpha, \lambda_3^\alpha), \quad (16)$$

for any $\alpha > 0$. It is worth noting that the Seth-Hill material family [Seth 1964] has a parameter that controls nonlinearity. Our non-linearization has been inspired by this family, and could be seen as its natural generalization to an arbitrary hyperelastic isotropic material. As a matter of fact, the Seth-Hill family is a special case of our method, namely when our method is applied to the Linear Corotational material. As an important example, the StVK material is obtained from the Linear Corotational material for $\alpha = 2$. This explains why film VFX practitioners have observed that the StVK material is “stiffer” (more nonlinear; it progressively stretches less

Table 1. **Common 3D volumetric elastic materials and their linear parameters.** We have $J = \lambda_1 \lambda_2 \lambda_3$.

Name	$\Psi(\lambda_1, \lambda_2, \lambda_3)$	$\lambda_{\text{Lamé}}$	$\mu_{\text{Lamé}}$
Linear Corotational (S.H. $\alpha = 1$)	$\mu(\sum_{i=1}^3 (\lambda_i - 1)^2) + \frac{\lambda}{2}(-3 + \sum_{i=1}^3 \lambda_i)^2$	λ	μ
St. Venant-Kirchhoff (S.H. $\alpha = 2$)	$\frac{\mu}{4}(\sum_{i=1}^3 (\lambda_i^2 - 1)^2) + \frac{\lambda}{8}(-3 + \sum_{i=1}^3 \lambda_i^2)^2$	λ	μ
Hencky (S.H. $\alpha = 0$)	$\mu(\sum_{i=1}^3 \log^2 \lambda_i) + \frac{\lambda}{2} \log^2 J$	λ	μ
Seth-Hill family (S.H.) [Seth 1964]	$\frac{\mu}{4}(\sum_{i=1}^3 (\lambda_i^\alpha - 1)^2) + \frac{\lambda}{2\alpha^2}(-3 + \sum_{i=1}^3 \lambda_i^\alpha)^2$	λ	μ
Symmetric Seth-Hill [Bazant 1998]	$\frac{\mu}{4\alpha^2}(\sum_{i=1}^3 (\lambda_i^\alpha - \frac{1}{\lambda_i^\alpha})^2) + \frac{\lambda}{8\alpha^2}(\sum_{i=1}^3 (\lambda_i^\alpha - \frac{1}{\lambda_i^\alpha}))^2$	λ	μ
Hill family [Hill 1968]	$\mu(\sum_{i=1}^3 f^2(\lambda_i)) + \frac{\lambda}{2}(\sum_{i=1}^3 f(\lambda_i))^2$	λ	μ
Neo-Hookean (standard version)	$\frac{\mu}{2}(-3 + \sum_{i=1}^3 \lambda_i^2) - \mu \log J + \frac{\lambda}{2} \log^2 J$	λ	μ
Neo-Hookean (Ogden)	$\frac{\mu}{2}(-3 + \sum_{i=1}^3 \lambda_i^2) - \mu \log J + \frac{\lambda}{2}(J - 1)^2$	λ	μ
Stable Neo-Hookean (Eq. 13 in [Smith et al. 2018])	$\frac{\mu}{2}(-3 + \sum_{i=1}^3 \lambda_i^2) - \mu(J - 1) + \frac{\lambda}{2}(J - 1)^2$	$\lambda - \mu$	μ
STS material [Pai et al. 2018]	$\frac{\mu}{2}(-3 + \sum_{i=1}^3 \lambda_i^2) - \mu \log J + \frac{\lambda}{2} \log^2 J + \frac{\mu\lambda}{8}(\sum_{i=1}^3 (\lambda_i^2 - 1)^4)$	λ	μ
Valanis-Landel (original) [Valanis and Landel 1967]	$2\mu \sum_{i=1}^3 \lambda_i (\log \lambda_i - 1) + \frac{\lambda}{2} \log^2 J$	λ	μ
Valanis-Landel (new) [Chen et al. 2023; Valanis 2022]	$\sum_{i=1}^3 f(\lambda_i) + h(J)$	$h''(1)$	$\frac{1}{2} f''(1)$
Valanis-Landel (Xu's version) [Xu et al. 2015]	$\sum_{i=1}^3 f(\lambda_i) + \sum_{i,j=1}^3 g(\lambda_i \lambda_j) + h(J)$	$g''(1) + h''(1)$	$\frac{1}{2}(f''(1) + g''(1))$
Peng-Landel [Peng and Landel 1972]	$E \sum_{i=1}^3 (\lambda_i - 1 - \log \lambda_i - \frac{1}{6} \log^2 \lambda_i + \frac{1}{18} \log^3 \lambda_i - \frac{1}{216} \log^4 \lambda_i)$	0	$\frac{E}{3}$
ARAP (As-Rigid-As-Possible) [Sorkine and Alexa 2007]	$\ F - R\ ^2 = \sum_{i=1}^3 (\lambda_i - 1)^2$	0	1
Symmetric ARAP [Shtengel et al. 2017]	$\frac{\mu}{2}(\ F - R\ ^2 + \ F^{-1} - R^{-1}\ ^2) = \frac{\mu}{2} \sum_{i=1}^3 ((\lambda_i - 1)^2 + (1 - \frac{1}{\lambda_i})^2)$	0	μ
Symmetric Dirichlet [Smith and Schaefer 2015]	$\frac{1}{2}(\ F\ ^2 + \ F^{-1}\ ^2) = \frac{1}{2} \sum_{i=1}^3 (\lambda_i - \frac{1}{\lambda_i})^2$	0	2
Ogden [Ogden 1972]	$\sum_{p=1}^N \frac{\mu_p}{\alpha_p} (-3 + \sum_{i=1}^3 \lambda_i^{\alpha_p})$	0	$\frac{1}{2} \sum_{p=1}^N \mu_p (\alpha_p - 1)$
Mooney-Rivlin	$C_1 J^{\frac{-2}{3}} (-3 + \sum_{i=1}^3 \lambda_i^2) + C_2 J^{\frac{-4}{3}} (-3 + \sum_{i=1}^3 \lambda_i^2 \lambda_{1+(i \bmod 3)}^2)$	$-\frac{4}{3}(2C_1 + 5C_2)$	C_1

and less when force is increased) under large deformations than the Linear Corotational material, and is as such more suitable for modeling biological tissues [Barbič 2024].

The gradient and Hessian of ψ_α can be easily computed

$$\nabla \psi_\alpha(\lambda_1, \lambda_2, \lambda_3) = \frac{1}{\alpha} \begin{pmatrix} \lambda_1^{\alpha-1} \partial_1 \psi(\lambda_1^\alpha, \lambda_2^\alpha, \lambda_3^\alpha) \\ \lambda_2^{\alpha-1} \partial_2 \psi(\lambda_1^\alpha, \lambda_2^\alpha, \lambda_3^\alpha) \\ \lambda_3^{\alpha-1} \partial_3 \psi(\lambda_1^\alpha, \lambda_2^\alpha, \lambda_3^\alpha) \end{pmatrix}, \quad (17)$$

$$\nabla^2 \psi_\alpha(\lambda_1, \lambda_2, \lambda_3) = \frac{\alpha-1}{\alpha} \text{diag}(\lambda_1^{\alpha-2} \partial_1 \psi, \lambda_2^{\alpha-2} \partial_2 \psi, \lambda_3^{\alpha-2} \partial_3 \psi) + \begin{pmatrix} \lambda_1^{2\alpha-2} \partial_{11} \psi & \lambda_1^{\alpha-1} \lambda_2^{\alpha-1} \partial_{12} \psi & \lambda_1^{\alpha-1} \lambda_3^{\alpha-1} \partial_{13} \psi \\ \lambda_1^{\alpha-1} \lambda_2^{\alpha-1} \partial_{12} \psi & \lambda_2^{2\alpha-2} \partial_{22} \psi & \lambda_2^{\alpha-1} \lambda_3^{\alpha-1} \partial_{23} \psi \\ \lambda_1^{\alpha-1} \lambda_3^{\alpha-1} \partial_{13} \psi & \lambda_2^{\alpha-1} \lambda_3^{\alpha-1} \partial_{23} \psi & \lambda_3^{2\alpha-2} \partial_{33} \psi \end{pmatrix}. \quad (18)$$

Plugging the rest shape $\lambda_1 = \lambda_2 = \lambda_3 = 1$ into Equation 18, one can easily see that $\nabla^2 \psi_\alpha(1, 1, 1) = \nabla^2 \psi(1, 1, 1)$. Therefore, the PK1-linearization remains the same. Observe that for $\alpha < 1$, $\alpha = 1$, $\alpha > 1$ the material softens, remains the same, and stiffens under large deformations, respectively. Figures 2 and 3 demonstrate the effect of tweaking α . Note that applying the nonlinearization is very easy and requires minimal coding change; all is needed is to add the α parameter to the existing code and minimally modify the classes that compute the elastic energy, its gradient and Hessian, as given in Equation 16, 17, and 18.

6 MIXING AND MATCHING MATERIALS

For many materials, the elastic energy ψ is already separated into the “ $\lambda_{\text{Lamé}}$ ” and “ $\mu_{\text{Lamé}}$ ” parts (e.g. Seth-Hill family, the Neo-Hookean materials, STS material, and the original and “new” Valanis-Landel material; see Table 1),

$$\psi(\lambda_1, \lambda_2, \lambda_3) = \lambda_{\text{Lamé}} \psi_{\lambda_{\text{Lamé}}}(\lambda_1, \lambda_2, \lambda_3) + \mu_{\text{Lamé}} \psi_{\mu_{\text{Lamé}}}(\lambda_1, \lambda_2, \lambda_3), \quad (19)$$

where the $\lambda_{\text{Lamé}}$ and $\mu_{\text{Lamé}}$ of $\psi_{\lambda_{\text{Lamé}}}$ (as defined in Equation 3) are 1 and 0, respectively, and the $\lambda_{\text{Lamé}}$ and $\mu_{\text{Lamé}}$ of $\psi_{\mu_{\text{Lamé}}}$ (as defined in Equation 4) are 0 and 1, respectively. This makes it possible to produce new materials by linearly combining $\psi_{\lambda_{\text{Lamé}}}$ and $\psi_{\mu_{\text{Lamé}}}$ from two distinct materials, producing new materials. These materials are sometimes superior to the original materials. For example, $\psi_{\lambda_{\text{Lamé}}}$ of Linear Corotational and StVK materials only provide volume preservation (at the selected ν) for small deformations. Under large deformation, those formulas no longer corresponds to any kind of volume preservation. To address this, one can combine $\psi_{\mu_{\text{Lamé}}}$ of either of those materials with the $\psi_{\lambda_{\text{Lamé}}}$ of a Neo-Hookean material (essentially either $(J-1)^2$ or $\log^2(J)$). This produces a material that obeys the Poisson’s effect of the given ν under small deformations, but still preserve volume under large deformations. Although such materials have been proposed before (Linear Corotational with $(J-1)^2$ [Smith

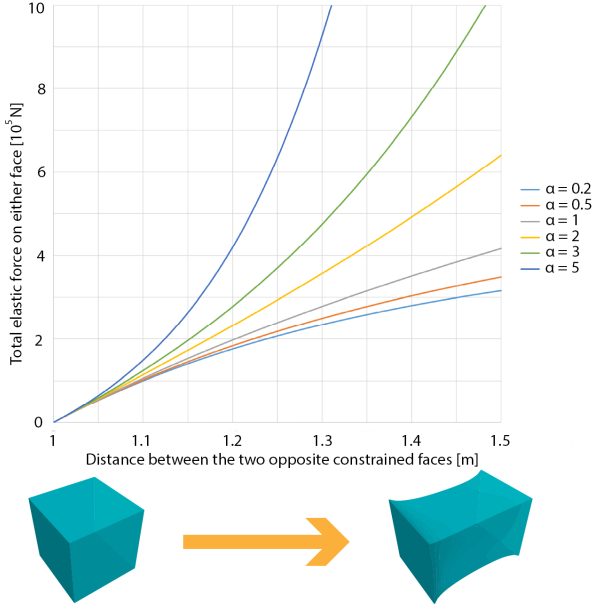


Fig. 3. **Modifying the nonlinearity of the Stable Neo-Hookean (SNH) material.** An elastic cube ($1\text{m} \times 1\text{m} \times 1\text{m}$) is constrained on two opposite faces and pulled apart. We plot the total elastic force on either face versus the distance between the two faces. Note that the distance is 1.0 when the cube is undeformed. The SNH material ($\alpha = 1$) is known to be “soft” under large deformations; observe that the curve is concave in this case. By adjusting α , SNH can be transformed into a much stiffer or softer material. Observe that all materials are the same in the linear region; this is thanks to using Equation 16 that preserves linear properties.

et al. 2018; Stomakhin et al. 2012]; StVK with $(J - 1)^2$ [Zheng et al. 2022]) our paper makes it possible to discover such combinations systematically. Also, our approach makes it possible to augment any energy that did not consider volume preservation. For example, we can augment geometry processing energies with volume preservation, giving them the ability to use a non-zero ν . Another example are incompressible materials in engineering literature. Commonly, the process of creating such materials works as follows. First, define an energy function ψ without any consideration for incompressibility (i.e., $\lambda_{\text{Lamé}} = \nu = 0$). Next, enforce exact incompressibility at the solver level, using constraints [Sussman and Bathe 2009; Valanis and Landel 1967]. We can take that same energy function ψ , and add a volume-preserving term $\psi_{\lambda_{\text{Lamé}}}$ of a Neo-Hookean material, with $\lambda_{\text{Lamé}}$ tuned using our Equation 3. This produces a compressible version of the same material that obeys the Poisson’s effect of the given ν .

Similarly, we can apply the nonlinearity idea separately to each part, using two independently tweakable parameters α_1 and α_2 ,

$$\begin{aligned} \psi_{\alpha_1, \alpha_2}(\lambda_1, \lambda_2, \lambda_3) &= \frac{\lambda_{\text{Lamé}}}{\alpha_1^2} \psi_{\lambda_{\text{Lamé}}}(\lambda_1^{\alpha_1}, \lambda_2^{\alpha_1}, \lambda_3^{\alpha_1}) + \\ &+ \frac{\mu_{\text{Lamé}}}{\alpha_2^2} \psi_{\mu_{\text{Lamé}}}(\lambda_1^{\alpha_2}, \lambda_2^{\alpha_2}, \lambda_3^{\alpha_2}). \end{aligned} \quad (20)$$

7 RESULTS

We implemented our results on a 3.00 GHz Intel Xeon i7 CPU E5-2687W v4 processor with 48 cores. The effect of applying the non-linearization to computation times is negligible. Our results enable the artist to adjust both the small-strain (rotation-aware) behavior as well as nonlinear behavior under large deformations. The dinosaur example (Figure 1) illustrates our contribution of adjusting the PK1-linearization behavior of elastic 3D solids. In this manner, two materials can be made to have equal behavior under small deformations, enabling one to more easily compare their nonlinearities under large deformations. Figures 2 and 3 demonstrate the effect of adjusting nonlinearity.

8 CONCLUSION

While the Linear Corotational material is widely used, we provided a formal framework and proved in it that this material is “special” and arguably the simplest kind of an isotropic material. We provided an algorithm to approximate any isotropic material with its “PK1-linearization”, namely the Linear Corotational material that shares the same Lamé parameters, or equivalently, the same Young’s modulus and Poisson’s ratio. We analytically derived the PK1-linearizations for many common materials (Table 1), and gave a method to minimally modify any material so that it has a desired target PK1-linearization. Finally, we demonstrated how to easily adjust the material nonlinearity using an intuitive one-dimensional parameter family, while keeping PK1-linearization constant. This makes it possible for artists to easily adjust both the small-deformation “stiffness” and volume preservation of a material, as well as adjust the rate at which the material stiffens or softens under large deformations. Arguably, such a 3-dimensional family provides very good modeling power for many digital artists, while retaining simplicity of having a very small number of parameters. Of course, nonlinearity is much more than just tweaking one parameter, and we did not investigate how nonlinearity could be adjusted by using several (more than two) meaningful parameters. Our volume preservation is controlled via the Poisson’s ratio ν , and as such the Poisson’s effect is only accurate under small deformations. Under large deformations Poisson’s ratio loses its meaning; this is commonly the case in nonlinear deformable object simulation and not a specific limitation of our method. That said, we proposed the “mixing and matching” method of using Neo-Hookean volume preservation with other “standard” volumetric materials, which ensures that the resulting material obeys the Poisson’s effect for any ν for small deformations, and still preserves volume under large deformations. In the future, we would like to investigate more general nonlinearity “filtering” functions other than the ones used in Equation 16 to achieve higher-order nonlinearity effects.

ACKNOWLEDGMENTS

This research was sponsored in part by NSF (IIS-1911224), USC Annenberg Fellowship to Huan Yu Chen, Bosch Research and Adobe Research.

REFERENCES

Veronica E Arriola-Rios, Puren Guler, Fanny Ficuciello, Danica Kragic, Bruno Siciliano, and Jeremy L Wyatt. 2020. Modeling of deformable objects for robotic manipulation:

- A tutorial and review. *Frontiers in Robotics and AI* 7 (2020), 82.
- J. Barbič. 2024. Personal correspondence with a leading VFX studio.
- Zdenek P Bazant. 1998. Easy-to-compute tensors with symmetric inverse approximating Hencky finite strain and its rate. (1998).
- Tibi Beda. 2014. An approach for hyperelastic model-building and parameters estimation a review of constitutive models. *European Polymer Journal* 50 (2014), 97–108.
- I. Chao, U. Pinkall, P. Sanan, and P. Schröder. 2010. A Simple Geometric Model for Elastic Deformations. *ACM Trans. on Graphics (SIGGRAPH 2010)* 29, 3 (2010), 38:1–38:6.
- Huanyu Chen, Danyong Zhao, and Jernej Barbič. 2023. Capturing Animation-Ready Isotropic Materials Using Systematic Poking. *ACM Trans. on Graphics (SIGGRAPH Asia 2023)* 42, 6 (2023).
- Hong He, Qiang Zhang, Yaru Zhang, Jianfeng Chen, Liqun Zhang, and Fanzhu Li. 2022. A comparative study of 85 hyperelastic constitutive models for both unfilled rubber and highly filled rubber nanocomposite material. *Nano Materials Science* 4, 2 (2022), 64–82.
- Florian Hecht, Yeon Jin Lee, Jonathan R. Shewchuk, and James F. O’Brien. 2012. Updated sparse cholesky factors for corotational elastodynamics. *ACM Trans. Graph.* 31, 5, Article 123 (2012), 13 pages.
- R Hill. 1968. On constitutive inequalities for simple materials—I. *Journal of the Mechanics and Physics of Solids* 16, 4 (1968), 229–242.
- G. Irving, J. Teran, and R. Fedkiw. 2004. Invertible Finite Elements for Robust Simulation of Large Deformation. In *Symp. on Computer Animation (SCA)*. 131–140.
- Theodore Kim and David Eberle. 2020. Dynamic Deformables: Implementation and Production Practicalities. In *ACM SIGGRAPH 2020 Courses*.
- A. McAdams, Y. Zhu, A. Selle, M. Empey, R. Tamstorf, J. Teran, and E. Sifakis. 2011. Efficient elasticity for character skinning with contact and collisions. *ACM Trans. on Graphics (SIGGRAPH 2011)* 30, 4 (2011), 37:1–37:11.
- Stephen K Melly, Liwu Liu, Yanju Liu, and Jinsong Leng. 2021. A review on material models for isotropic hyperelasticity. *International Journal of Mechanical System Dynamics* 1, 1 (2021), 71–88.
- M. Müller and M. Gross. 2004. Interactive Virtual Materials. In *Proc. of Graphics Interface 2004*. 239–246.
- Raymond William Ogden. 1972. Large deformation isotropic elasticity—on the correlation of theory and experiment for incompressible rubberlike solids. *Proceedings of the Royal Society of London. A. Mathematical and Physical Sciences* 326, 1567 (1972), 565–584.
- Dinesh K Pai, Austin Rothwell, Pearson Wyder-Hodge, Alistair Wick, Ye Fan, Egor Larionov, Darcy Harrison, Debanga Raj Neog, and Cole Shing. 2018. The human touch: measuring contact with real human soft tissues. *ACM Trans. on Graphics (ACM SIGGRAPH 2018)* 37, 4 (2018), 58.
- TJ Peng and RF Landel. 1972. Stored energy function of rubberlike materials derived from simple tensile data. *Journal of Applied Physics* 43, 7 (1972), 3064–3067.
- BR Seth. 1964. *Generalized strain measure with applications to physical problems*. United States Department of the Army Mathematics Research Center.
- Anna Shtengel, Roi Poranne, Olga Sorkine-Hornung, Shahar Z. Kovalsky, and Yaron Lipman. 2017. Geometric Optimization via Composite Majorization. *ACM Trans. on Graphics (SIGGRAPH 2017)* 36, 4, Article 38 (2017).
- Eftychios Sifakis and Jernej Barbič. 2012. FEM simulation of 3D deformable solids: a practitioner’s guide to theory, discretization and model reduction. In *ACM SIGGRAPH 2012 Courses*. 20:1–20:50.
- B. Smith, F. De Goes, and T. Kim. 2018. Stable Neo-Hookean Flesh Simulation. *ACM Trans. Graph.* 37, 2 (2018), 12:1–12:15.
- Jason Smith and Scott Schaefer. 2015. Bijective Parameterization with Free Boundaries. *ACM Trans. on Graphics (SIGGRAPH 2015)* 34, 4, Article 70 (2015).
- Olga Sorkine and Marc Alexa. 2007. As-rigid-as-possible surface modeling. In *Symposium on Geometry processing*, Vol. 4. Citeseer, 109–116.
- Alexey Stomakhin, Russell Howes, Craig Schroeder, and Joseph M. Teran. 2012. Energetically Consistent Invertible Elasticity. In *Symp. on Computer Animation (SCA)*. 25–32.
- Theodore Sussman and Klaus-Jürgen Bathe. 2009. A model of incompressible isotropic hyperelastic material behavior using spline interpolations of tension-compression test data. *Communications in Numerical Methods in Engineering* 25, 1 (2009), 53–63.
- Joseph Teran, Eftychios Sifakis, Geoffrey Irving, and Ronald Fedkiw. 2005. Robust Quasistatic Finite Elements and Flesh Simulation. In *Symp. on Computer Animation (SCA)*. 181–190.
- KC Valanis and Robert F Landel. 1967. The strain-energy function of a hyperelastic material in terms of the extension ratios. *Journal of Applied Physics* 38, 7 (1967), 2997–3002.
- Kirk C Valanis. 2022. The Valanis–Landel strain energy function Elasticity of incompressible and compressible rubber-like materials. *International Journal of Solids and Structures* 238 (2022), 111271.
- Mickeal Verschoor, Daniel Lobo, and Miguel A Otaduy. 2018. Soft hand simulation for smooth and robust natural interaction. In *IEEE Conf. on Virtual Reality and 3D User Interfaces (VR)*. 183–190.
- Bohan Wang, Yili Zhao, and Jernej Barbič. 2017. Botanical Materials Based on Biomechanics. *ACM Trans. on Graphics (SIGGRAPH 2017)* 36, 4 (2017).
- Bohan Wang, Mianlun Zheng, and Jernej Barbič. 2020. Adjustable Constrained Soft-Tissue Dynamics. *Pacific Graphics 2020 and Computer Graphics Forum* 39, 7 (2020).
- Hongyi Xu, Funshing Sin, Yufeng Zhu, and Jernej Barbič. 2015. Nonlinear material design using principal stretches. *ACM Trans. on Graphics (SIGGRAPH 2015)* 34, 4 (2015), 1–11.
- Mianlun Zheng, Bohan Wang, Jingtao Huang, and Jernej Barbič. 2022. Simulation of Hand Anatomy Using Medical Imaging. *ACM Trans. on Graphics (SIGGRAPH Asia 2022)* 41, 6 (2022).